

# Evaluation of excitation energy and spin from light charged particles multiplicities in heavy-ion collisions

J.C. Steckmeyer<sup>1\*</sup>, Z. Sosin<sup>2</sup>, K. Grotowski<sup>2,3</sup>, P. Pawłowski<sup>3</sup>,  
S. Aiello<sup>4</sup>, A. Anzalone<sup>5</sup>, M. Bini<sup>6</sup>, B. Borderie<sup>7</sup>, R. Bougault<sup>1</sup>,  
G. Cardella<sup>4</sup>, G. Casini<sup>6</sup>, S. Cavallaro<sup>5</sup>, J.L. Charvet<sup>8</sup>, R. Dayras<sup>8</sup>,  
E. De Filippo<sup>4</sup>, D. Durand<sup>1</sup>, S. Feminò<sup>9</sup>, J.D. Frankland<sup>10</sup>, E. Galichet<sup>7,11</sup>,  
M. Geraci<sup>4</sup>, F. Giustolisi<sup>5</sup>, P. Guazzoni<sup>12</sup>, M. Iacono Manno<sup>5</sup>, G. Lanzalone<sup>5</sup>,  
G. Lanza<sup>4</sup>, N. Le Neindre<sup>7</sup>, S. Lo Nigro<sup>4</sup>, F. Lo Piano<sup>5</sup>, A. Olmi<sup>6</sup>,  
A. Pagano<sup>4</sup>, M. Papa<sup>5</sup>, M. Parlog<sup>13</sup>, G. Pasquali<sup>6</sup>, S. Piantelli<sup>6</sup>,  
S. Pirrone<sup>4</sup>, G. Politi<sup>4</sup>, F. Porto<sup>5</sup>, M.F. Rivet<sup>7</sup>, F. Rizzo<sup>5</sup>, E. Rosato<sup>14</sup>,  
R. Roy<sup>15</sup>, S. Sambataro<sup>4†</sup>, M.L. Sperduto<sup>4</sup>, A.A. Stefanini<sup>6</sup>, C. Sutura<sup>4</sup>,  
B. Tamain<sup>1</sup>, E. Vient<sup>1</sup>, C. Volant<sup>8</sup>, J.P. Wieleczko<sup>10</sup> and L. Zetta<sup>12</sup>  
(The INDRA and CHIMERA collaborations)

<sup>1</sup>LPC, IN2P3-CNRS, ENSICAEN et Université de Caen, 14050 Caen-cedex 04, France.

<sup>2</sup>Institute of Physics, Jagellonian University, Reymonta 4, 30-059 Kraków, Poland.

<sup>3</sup>Institute of Nuclear Physics PAN, Radzikowskiego 152, 31-342 Kraków, Poland.

<sup>4</sup>INFN Sezione di Catania and Dipartimento di Fisica e Astronomia, Università di Catania, 95123 Catania, Italy.

<sup>5</sup>LNS and Dipartimento di Fisica e Astronomia, Università di Catania, 95123 Catania, Italy.

<sup>6</sup>INFN e Università di Firenze, 50125 Firenze, Italy.

<sup>7</sup>Institut de Physique Nucléaire, IN2P3-CNRS, 91406 Orsay-cedex, France.

<sup>8</sup>DAPNIA/SPhN, CEA/Saclay, 91191 Gif-sur-Yvette-cedex, France.

<sup>9</sup>INFN e Università di Messina, 98100 Messina, Italy.

<sup>10</sup>GANIL, CEA et IN2P3-CNRS, BP 5027, 14076 Caen-cedex 05, France.

<sup>11</sup>CNAM, Laboratoire des Sciences Nucléaires, 2 rue Conté, 75003 Paris, France.

<sup>12</sup>INFN e Università di Milano, 20133 Milano, Italy.

<sup>13</sup>National Institute for Physics and Nuclear Engineering, Bucharest-Magurele, Romania.

<sup>14</sup>INFN e Dipartimento di Scienze Fisiche, Università di Napoli "Federico II", Napoli, Italy.

<sup>15</sup>Laboratoire de Physique Nucléaire, Université Laval, Québec, Canada.

## Abstract

A simple procedure for evaluating the excitation energy and the spin transfer in heavy-ion dissipative collisions is proposed. It is based on a prediction of the GEMINI evaporation code : for a nucleus with a given excitation energy, the average number of emitted protons decreases with increasing spin, whereas the average number of alpha particles increases. Using that procedure for the reaction  $^{107}\text{Ag}+^{58}\text{Ni}$  at 52 MeV/nucleon, the excitation energy and spin of quasi-projectiles have been evaluated. The results obtained in this way have been compared with the predictions of a model describing the primary dynamic stage of heavy-ion collisions.

---

\*Corresponding author, e-mail address : Jean-Claude.Steckmeyer@lpccaen.in2p3.fr, tel : +33 2 31 45 29 66, fax : +33 2 31 45 25 49

†deceased

PACS: 25.70.-z, 25.70.Lm, 25.60.Mn

Keywords: Nuclear reactions  $^{107}\text{Ag}(^{58}\text{Ni}+\text{X})$ ,  $E = 52 \text{ A.MeV}$ , heavy-ion interactions, peripheral reactions, projectile deexcitation, excitation energy, angular momentum transfer, transport model calculations.

In intermediate energy heavy-ion collisions at large impact parameters, a significant part of the initial kinetic energy is converted into heat inside the partners moving away from each other in the exit channel. Nucleon exchange as well as nucleon-nucleon (NN) collisions are responsible for the dissipation of energy, creating two main excited fragments namely the quasi-projectile (QP) and the quasi-target (QT) [1]. Meanwhile, a fraction of the initial orbital angular momentum is transferred into intrinsic angular momentum (or spin) of the fragments.

Decaying QP's and QT's are observed as sources of nucleons, light charged particles (LCP's), intermediate mass fragments (IMF's) or fission fragments for heavier systems, and  $\gamma$ -rays. Besides, a third source of particles appears in the region between the QP and QT fragments (see e.g. [2, 3, 4]). The contribution of such an intermediate velocity source (IVS) depends on the initial angular momentum and masses of the colliding nuclei in the entrance channel.

Production of excited nuclei with large spins and large excitation energies is important to study the de-excitation properties of hot nuclear matter. In particular, the role of angular momentum in the multifragmentation process has been emphasized [5]. The nucleus spin is usually evaluated from the angular distribution of the emitted products. Measurements using  $\gamma$ -rays [6], LCP's [7] and fission fragments [8] have been performed mainly at low bombarding energies, but scarce measurements exist in the intermediate energy range [9, 10]. In this Letter, we propose a simple procedure for evaluating the excitation energy and spin transfer in heavy-ion dissipative collisions.

Binary dissipative collisions in the  $^{107}\text{Ag}+^{58}\text{Ni}$  reaction have been studied at GANIL in inverse kinematics using a  $^{107}\text{Ag}$  beam at 52 MeV/nucleon [11]. For that purpose, the standard INDRA setup [12] was modified to detect QT nuclei recoiling with low kinetic energies of typically a few tens of MeV. Ten large area ( $5\times 5 \text{ cm}^2$ ) Si detectors, each of them having four vertical strips, were used for the detection of QT nuclei in discrete angular domains ranging from  $3^\circ$  to  $87^\circ$ . They were placed in the horizontal plane of INDRA. The mass of the secondary QT (QT residue) was deduced from energy and time-of-flight (TOF) measurements. As in the 52 MeV/nucleon  $^{107}\text{Ag}+^{58}\text{Ni}$  reaction the QP is expected to be emitted at very forward angles, the first ring of the INDRA detector made of 12 phoswich plastic scintillators ( $2^\circ < \theta < 3^\circ$ ) was replaced by the first wheel of the CHIMERA detector [13], mounted at a distance of 4 m from the target in a dedicated vacuum chamber. The CHIMERA detectors consisted of 2 rings of 16 Si detector - CsI scintillator telescopes, allowing for a better identification of the atomic number of the secondary QP (QP residue) in the angular range  $1^\circ < \theta < 3^\circ$ . Event acquisition was triggered by the detection of a charged product in one of the 10 TOF-Si detectors. The binary events were selected by requiring that the mass of that nucleus, assumed to be the QT residue, be larger than 20 u. Such conditions selected peripheral and semi-peripheral collisions. Only complete events were kept in the analysis: events with total detected charge and momentum larger than 90 % of the incident charge and momentum, respectively. In the following we will concentrate in studying the properties of the primary QP. It has been reconstructed with particles emitted in its forward hemisphere, their contribution being counted twice. In doing so, most of particles emitted from other sources are assumed being not accounted for. For the data set considered in this work, the reconstructed average primary QP charge is  $47\pm 2$ .

Let  $E^*/A$  and  $J$  denote the excitation energy per nucleon and spin of the primary QP, respectively. For the purpose of the  $E^*/A$  and  $J$  evaluation procedure (in this paper referred to as the *procedure*), the Monte-Carlo code GEMINI [14] was used to simulate the de-excitation stage of the primary QP. Standard prescriptions were used with a temperature dependent level density parameter [15]. In the framework of that model and for a given nucleus, the knowledge of the average proton and alpha particle multiplicities,  $\overline{M}_p$  and  $\overline{M}_\alpha$ , makes possible the estimation of the excitation energy and spin of that nucleus: a given  $(\overline{M}_p, \overline{M}_\alpha)$  couple corresponds to a unique  $(E^*/A, J)$  couple. Such a determination is valid as long as the multiplicities predicted by GEMINI are not too far from the experimental values, and the considered particles really come from

the nucleus under study. Similar attempts were made to determine the fragment spin by looking at the ratio of H to He isotopes [16].

The multiplicity of IMF's emitted by the primary QP is low compared to that of LCP's [11] : in the most dissipative collisions studied here,  $\overline{M}_p$ ,  $\overline{M}_\alpha$  and  $\overline{M}_{IMF}$  are 1.71, 1.19 and 0.16, respectively, in the forward hemisphere. Consequently, the GEMINI calculations will be performed allowing only for neutron and LCP evaporation (hydrogen and helium nuclei) and no IMF emission. Since among the LCPs, the  $^1\text{H}$  and  $^4\text{He}$  isotopes prevail, further on we will mention mainly protons and alpha particles.

As predicted by GEMINI, both  $\overline{M}_p$  and  $\overline{M}_\alpha$  increase with increasing excitation energy. However, for a given excitation energy,  $\overline{M}_p$  decreases with increasing spin, whereas  $\overline{M}_\alpha$  increases, i.e. the higher the spin, the heavier the mass of the evaporated particle. Indeed, the best way for a fast rotating nucleus to release its spin is to emit heavy ejectiles which carry away high angular momentum. Such an effect of the nucleus spin on the probability of particle evaporation has also been seen in [17]. This opposite behavior of  $\overline{M}_p$  as compared to  $\overline{M}_\alpha$  has been used in the *procedure* to extract the correlation between the excitation energy and the spin of the primary QP. GEMINI predictions can be used to draw the  $E^*/A$  vs.  $J$  curve associated with a constant  $\overline{M}_p$ , whatever the multiplicity of other LCP's. The same can be done for a constant  $\overline{M}_\alpha$  multiplicity. As shown in Fig. 1, these two curves exhibit an opposite trend, their intersection point defining the  $E^*/A$  and  $J$  values. Using this correspondence one can associate  $(E^*/A, J)$  values to each  $(\overline{M}_p, \overline{M}_\alpha)$  pair measured in the experiment.

In order to find out the evolution of  $E^*/A$  and  $J$  of the primary QP as a function of the dissipation, the events were sorted according to the QP residue velocity parallel to the beam, determined from the energy and the mass estimated from a fit performed on the stability valley. The associated velocity spectrum has been divided in twelve bins of equal width, going from 0.88 to 0.99 times the projectile velocity  $V_P$ . For these bins the  $\overline{M}_p$  and  $\overline{M}_\alpha$  multiplicities have been measured and the  $E^*/A$  and  $J$  values have been evaluated using the *procedure* shown in Fig. 1. GEMINI calculations were performed for a  $^{107}\text{Ag}$  nucleus because the reconstructed primary QP has a mean atomic number of 47, as mentioned previously. No attempt was made to account for the slight variation of the mean value of the atomic number as a function of the QP velocity nor for the width of its distribution. Such an analysis is beyond the scope of this work, mainly focused on the gross properties of the QP.

In the GEMINI calculations, at any given excitation energy, the charge of the QP residue  $Z_{QP}^{res}$  is found to be practically independent of the spin of the primary QP, suggesting that one can determine the excitation energy of the primary QP from the measurement of  $Z_{QP}^{res}$  [11]. Such a determination is presented as triangles in Fig. 2. The error bars displayed at QP residue velocities of .88-.89  $V_P$  and .94-.95  $V_P$  are estimates of the uncertainty on the  $E^*/A$  linked to an uncertainty of 2 charge units on the charge of the primary QP. The excitation energy can also be deduced from the experiment by using the calorimetry method [19] : the excitation energy of the primary QP is deduced from the kinetic energies of the emitted particles. In this evaluation, the neutron emission has been estimated from the difference between the mass of the primary QP, assumed to have the same neutron to proton ratio as the projectile, and the masses of all de-excitation products [10]. As one can see, the results of the calorimetry method, displayed as the hatched band in Fig. 2, agree well with the results obtained from the atomic number of the QP residue. Also a reasonable agreement with the values deduced from the LCP multiplicities is to be noted in the same figure (open circles deduced from the  $\overline{M}_p$  and  $\overline{M}_\alpha$  multiplicities and open squares from  $\overline{M}_{Z=1}$  and  $\overline{M}_{Z=2}$  multiplicities). However, the results obtained from the  $Z_{QP}^{res}$  charge are slightly higher, particularly above  $\approx 2$  MeV/nucleon. The experimental charge  $Z_{QP}^{res}$  accounts for emission of LCP's as well as IMF's. From the experimental value  $Z_{QP}^{res}$  and using the  $E^*/A - Z_{QP}^{res}$  correlation as calculated with GEMINI (taking into account only LCP emission), we deduce, in some sense, the excitation energy of a primary QP having emitted both LCP's and IMF's; a fraction of the experimental charge loss  $\Delta Z = Z_{QP}^{prim} - Z_{QP}^{res}$  being associated with IMF emission. At variance, the  $E^*/A$  deduced from the LCP multiplicity measurements reflects the  $E^*/A$  of a primary QP having only emitted H and He isotopes, the excitation energy of which is slightly lower than the one of the same nucleus having emitted the same numbers of H and He isotopes

plus a few IMF's.

In Fig. 3, the open circles show the  $E^*/A - J$  correlation extracted from the  $(\overline{M}_p, \overline{M}_\alpha)$  experimental data and the open squares the same correlation extracted from the multiplicities of  $Z = 1$  and  $Z = 2$  particles, using the same *procedure*. As can be seen, the spin increases linearly with increasing excitation energy (except below  $\approx 1$  MeV/nucleon) and reaches values up to 70-80  $\hbar$  at excitation energies of 3-3.5 MeV/nucleon. This maximum value is of the order of magnitude of the angular momentum at which the fission barrier of a  $^{107}\text{Ag}$  nucleus vanishes as predicted by the Fast Rotating Liquid Drop Model [18].

The  $E^*/A - J$  thus extracted is compared to the prediction of the Sosin model [20], referred herein as the *model*. This *model* does not assume full thermalization of the system of colliding heavy ions. Instead, individual fragments (clusters) are thermally equilibrated. Therefore the state densities can be applied for determining the configuration probabilities.

In the *model* a two-stage reaction scenario is assumed for a heavy ion collision which finally creates "hot sources" of particles. In the first stage, some of the nucleons become active reaction participants either via mean field effects or via NN interactions. In the second stage, these active nucleons may undergo coalescence, be transferred to the target remnant, to the projectile remnant, or to some clusters created earlier. Alternatively, they may escape to the continuum. The two stages of the reaction scenario do not mean a time sequence, but only a factorization of the total probability of particular configurations of particle systems.

In the mean field mechanism, one of the nucleons of the projectile nucleus or target nucleus becomes an active participant when running across a potential window which opens in the region between the colliding heavy ions. Both size and time during which the window remains open depend on the proximity and relative velocity of the heavy ions along their classical Coulomb trajectories. These trajectories are calculated for the interaction potentials (Coulomb and nuclear).

In the NN mechanism the two nucleons, one from the projectile and the other one from the target, collide in their overlap zone, where - for collisions at high energy and/or at large impact parameters - the Pauli principle becomes less restrictive. The nucleons of such a pair become reaction participants. The probability of a NN collision depends on the cross-section of the NN interaction, the convolution of the projectile and the target nucleus densities in the overlap region, as well as on the available momentum space.

The nucleon transfer process is executed in a series of steps. A detailed description of this process is given in [20]. The cluster coalescence process is possible when two clusters running along their trajectories are being trapped in a potential well.

A separate problem concerns the distribution of the excitation energy available at each step of the nucleon transfer process. The total energy of the system is of course conserved along the chain of transfers, but the excitation energies of individual subsystems vary according to the particular reaction  $Q$  value. For a given step  $k$  of nucleon transfer, the summation of the ground state and kinetic energies of fragments with their interaction potentials calculated for the exit reaction channel provides a value of the total energy corresponding to the internal degrees of freedom (excitation energy) of the system after step  $k$ . After subtracting the total excitation energy of the step  $k - 1$ , one obtains the corresponding reaction  $Q$  value which is divided among all involved subsystems of mass  $A > 4$ , with probability proportional to the corresponding densities of states.

The orbital angular momenta and intrinsic spins of the primary reaction products are calculated from the angular momenta of all nucleons of the system. The angular momenta of the nucleons are calculated assuming a Fermi gas distribution and that the initial locations depend upon the mean field and the NN interaction mechanism.

The *model* described above, coupled to the GEMINI evaporation code, has been successfully applied for description of reactions in medium heavy systems [21, 22].

For the reaction studied in this paper, the QP mass predicted by the *model* is  $A = 107 \pm 4$  (peripheral collisions); the contribution of the IVS protons and alphas emission in the forward hemisphere in the reference frame of the primary QP varies from 5 to 10% (depending on the impact parameter). Note, that these *model* predictions justify the assumptions made in the reconstruction of the primary QP and the choice of a  $^{107}\text{Ag}$  nucleus in the GEMINI calculations for application of the *procedure*. However, energy is dissipated by the IVS. In the most dissipative collisions studied

in this work, the model predictions lead to an excitation energy of the primary QP of  $\approx 365$  MeV, whereas the energy associated with the IVS emission reaches  $\approx 445$  MeV. These results are quite in agreement with a recent analysis performed on the  $^{93}\text{Nb}+^{93}\text{Nb}$  reaction at 38 MeV/nucleon [23]. Looking in more details to the calculations, it appears that on average  $(20\pm 7)$  nucleons originate from the IVS, 60% of them coming from the QT nucleus nearly two times lighter than the QP one. This explains in some way the weak evolution of the QP mass as a function of the dissipation.

In the simulations presented below, we use predictions for the primary dynamic reaction stage without de-excitation of the primary fragments. We assume that the QP has reached thermal equilibrium (see e.g. [21]) and that the evaporation of particles does not change its parallel velocity, due to the forward-backward symmetry of the angular distribution of the emitted LCP in the QP frame. In consequence, the primary QP velocity should be, on average, equal to the QP residue velocity.

Predictions of the *model* for the  $E^*/A - J$  correlation of the primary QP are displayed as lines in Figs. 2 and 3. The solid line presents the *model* calculations when the events are sorted as a function of the QP residue velocity and the broken line (Fig. 3) when data are sorted as a function of the excitation energy, disregarding the QP residue velocity. The *model* predictions are in better agreement with the excitation energies (Fig. 2) obtained from the atomic number of the QP residue and from the calorimetry method, than with the ones obtained from average LCP multiplicities. It is likely due to the fact, as stated before, that the IMF's are implicitly accounted for in the estimation of the excitation energy. For the QP spin values, the agreement between the *model* and the *procedure* predictions is good in a broad range of excitation energies (Fig. 3). A noticeable discrepancy is observed only below 1 MeV/nucleon. It should be pointed out that the *model* assumes zero values for the projectile and target intrinsic spins, and therefore the QP spin should vanish in the zero-excitation-energy limit. It is really the case for the *model* (broken line), where calculations were sorted as a function of the primary QP excitation energy. Alternatively, when the calculations are sorted as a function of the QP residue velocity bins, the QP spin vanishes at about 0.5 MeV/nucleon for both the *model* and the *procedure*. Such an effect could be explained by fluctuations and correlations between the spin and the velocity generated by the reaction mechanism.

In this work, the excitation energy of quasi-projectiles produced in the  $^{107}\text{Ag}+^{58}\text{Ni}$  reaction at 52 MeV/nucleon has been estimated in two distinct manners : from the calorimetry method and from comparisons with GEMINI calculations, using either LCP multiplicities or QP residue charge. The dynamical Sosin model reproduces these results and the overall agreement gives confidence in the evaluation of the primary QP excitation energy. The  $E^*/A - J$  correlation is also well reproduced by the calculations, indicating that the *procedure* is a powerful tool to determine the excitation energy and spin of excited nuclei from LCP experimental multiplicities. The agreement between the calorimetry method and the Sosin model implies that the contribution of the IVS particles is low in the forward hemisphere in the QP frame, otherwise the LCP multiplicities should be higher and the excitation energy too. Dynamical calculations presented in this paper reproduce the features of the primary QP source, i.e. charge, excitation energy and spin. By looking at the de-excitation step and cluster formation and comparing with the data, it should be possible to evaluate precisely the characteristics and properties of the IVS contribution. It is also important to explain contribution of fluctuations and correlations in the reaction picture. These are the goals of a forthcoming paper.

#### Acknowledgements

We are grateful to R. Bassini, C. Boiano, C. Calí, M. D'Andrea, F. Fichera, N. Guidice, N. Guardone, D. Nicotra, B. Raine, C. Rapisavoli, G. Rizza, J. Ropert, J. Tillier, M. Tripon, S. Urso, J.L. Vignet and G. Wittwer for their invaluable help in performing both mechanical, electronic and acquisition coupling of the first ring of CHIMERA with INDRA.

## References

- [1] See, for example W.U. Schröder, Nucl. Phys. **A538** (1992) 439c.

- [2] P. Pawłowski et al., Phys. Rev. **C57** (1998)1771.
- [3] T. Lefort et al., Nucl. Phys. **A662** (2000) 397.
- [4] D. Doré et al., Phys. Rev. **C63** (2001) 034612.
- [5] A. Botvina and D.H.E Gross, Nucl. Phys. **A592** (1995) 257.
- [6] J.B. Natowitz et al., Phys. Rev. Lett. **40** (1978) 751; R.A. Dayras et al., Phys. Rev. **C22** (1980) 1485.
- [7] R.A. Babinet et al., Z. Phys. **A295** (1980) 153.
- [8] P. Dyer et al., Phys. Rev. Lett. **39** (1977) 392; J.C. Steckmeyer et al., Nucl. Phys. **A427** (1984) 357.
- [9] J. Colin et al., Nucl. Phys. **A593** (1995) 48, and references therein.
- [10] J.C. Steckmeyer et al., Nucl. Phys. **A686** (2001) 537.
- [11] J.C. Steckmeyer et al., Proc. of XL<sup>th</sup> International Winter Meeting on Nuclear Physics, Bormio, Italy, January 21-26, Edited by I. Iori, 2002, 198.
- [12] J. Pouthas et al., NIM **A357** (1995) 418; J. Pouthas et al., NIM **A369** (1996) 222.
- [13] A. Pagano et al. Nucl. Phys. **A734** (2004) 504.
- [14] R.J. Charity et al., Nucl. Phys. **A483** (1988) 371.
- [15] J. Lestone, Phys. Rev. **C52** (1995) 1118
- [16] G. Catchen et al., Phys. Rev. **C21** (1980) 940;  
G. Casini et al., Phys. Rev. Lett. **83** (1999) 2537;  
G. Casini et al., Eur. Phys. J. **A9** (2000) 491.
- [17] A. Di Pietro et al., Nucl. Phys. **A689** (2001) 668.
- [18] A.J. Sierk, Phys. Rev. **C33**(1986) 2039.
- [19] J. Péter et al., Nucl. Phys. **A593** (1995) 95.
- [20] Z. Sosin, Eur. Phys. J. **A11** (2001) 311.
- [21] R. Płaneta et al., Eur. Phys. J. **A11** (2001) 297;  
Z. Sosin et al., Eur. Phys. J. **A11** (2001) 305;  
R. Płaneta et al., Acta Phys. Polonica **B32** (2001) 3079.
- [22] A.M. Buta, Ph. D. Thesis, Université de Caen (2003), <http://tel.ccsd.cnrs.fr/documents/archives0/00/00/39/34/>
- [23] A. Mangiarotti et al., Phys. Rev. Lett. **93** (2004) 232701.

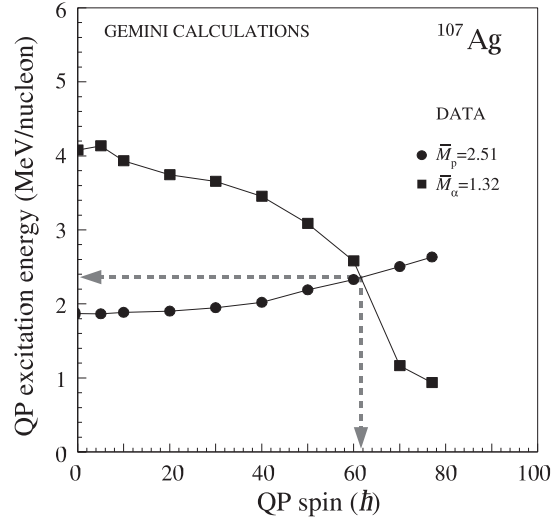


Figure 1:  $\overline{M}_p = \text{const}$  and  $\overline{M}_\alpha = \text{const}$  curves in the  $E^*/A$  excitation energy vs.  $J$  spin plane as generated by the GEMINI calculations.

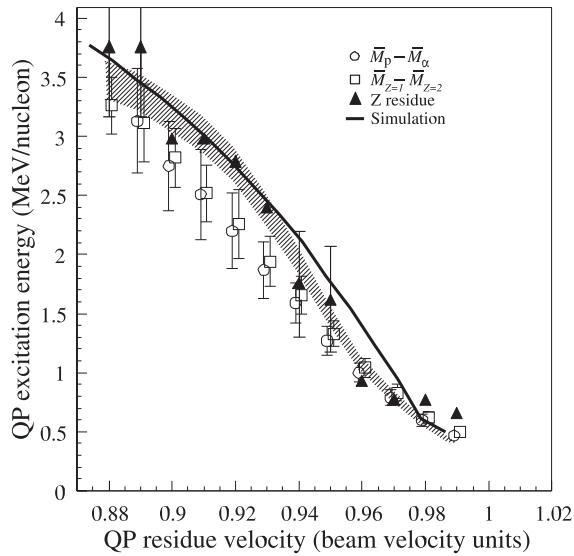


Figure 2: As a function of the QP residue velocity, the excitation energy of the primary QP deduced from the charge of the detected QP residue (black triangles), from the calorimetry method (hatched band) and from the  $(\overline{M}_p, \overline{M}_\alpha)$  and  $(\overline{M}_{Z=1}, \overline{M}_{Z=2})$  experimental data (open circles and squares).

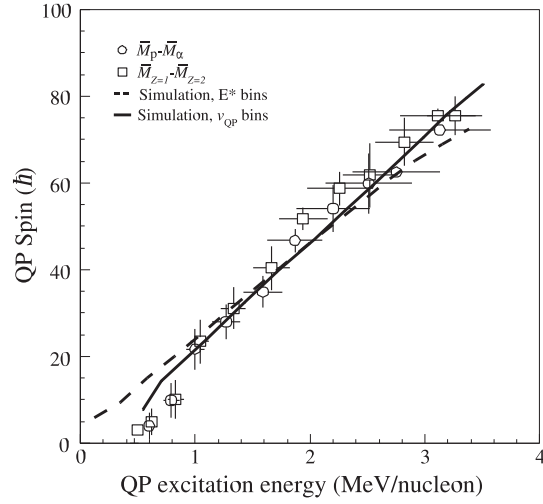


Figure 3: Spin of the primary quasi-projectile vs. its excitation energy. For open circles the proton and alpha particle multiplicities were used, and for open squares the multiplicities of  $Z = 1$  and  $Z = 2$  particles. Solid and broken lines denote model simulations. The solid line is the excitation energy - spin correlation obtained when data are sorted as a function of the QP residue velocity and the broken line when data are sorted as a function of the excitation energy.